Indonesian Review of Physics (IRiP)
Vol.8, No.2, Dec 2025, pp. 61 - 68

p-ISSN: 2621-3761 | e-ISSN: 2621-2889
DOI: 10.12928/irip.v8i2.16069

Non-Invasive Blood Glucose Estimation Using PPG Derivative Features and MFCCs with Random Forest

Ferdyan Rahmadani Adhi Pramudya, Muhammad Bagoes Anargiansyah, Bilqis Regita Pratiwi Fayensi, Moh Khikam Amrullah, Nisa'ul Fadhilah, Nainunis Mutawakkillah, Muhimmatul Khoiro*
Universitas Negeri Surabaya, Indonesia
Email: muhimmatulkhoiro@unesa.ac.id

Article Info

Article History
Received: Apr 1, 2026
Revision: May 5, 2026
Accepted: Jun 13, 2026

Keywords:
APG
Diabetes
Fiducial Features
MFCCs
Non-invasive

ABSTRACT

Conventional blood glucose measurement devices remain dominated by invasive methods that require direct contact with body tissues and cause patient discomfort, motivating the development of accurate and non-invasive blood glucose monitoring approaches. Therefore, blood glucose estimation has performed using Photoplethysmography (PPG) signals by exploiting the Velocity Photoplethysmogram (VPG) and the Acceleration Photoplethysmogram (APG) as derivative signals. PPG signals were acquired non-invasively from 58 participants using an optical MAX30102 sensor placed on the finger. Morphological fiducial features and Mel-Frequency Cepstral Coefficients (MFCCs) were extracted from PPG, VPG, and APG signals to capture temporal, morphological, and spectral characteristics related to peripheral hemodynamic changes. The extracted features were then used to model blood glucose levels using a Random Forest algorithm. The results showed that the combined use of PPG, VPG, and APG produced the best performance, achieving Mean Absolute Error (MAE), Root Mean Square Error (RMSE), and Mean Absolute Relative Difference (MARD) values of 6.35 mg/dL, 9.74 mg/dL, and 6.07%, respectively. Clarke Error Grid Analysis (CEGA) showed that 97.44% of the predictions were located in Zone A and 2.56% in Zone B, indicating that all estimates were within clinically acceptable regions. The main scientific contribution of this study lies in integrating derivative PPG signals with fiducial and MFCC-based feature representations within a unified machine learning framework. These findings indicate that combining PPG, VPG, and APG provides a richer physiological representation than PPG alone and offers practical potential for the development of wearable-based, non-invasive blood glucose monitoring technology.

To cite this article:
F. R. A. Pramudya *et al.*, "Non-Invasive Blood Glucose Estimation Using PPG Derivative Features and MFCCs with Random Forest," *Indones. Rev. Phys.*, vol. 8, no. 2, pp. 61–68, 2025, doi: 10.12928/irip.v8i2.16069

I. Introduction

Diabetes Mellitus (DM) is a chronic metabolic disorder that requires continuous monitoring of blood glucose levels to support effective disease management and prevent complications [1], [2], [3]. However, current clinical and daily monitoring practices still largely rely on invasive techniques that require direct blood sampling. These methods may cause discomfort and potentially reduce patient adherence, particularly during long-term or frequent monitoring [4], [5]. Therefore, non-invasive blood glucose monitoring has gained increasing attention as an alternative approach for estimating glucose levels

without damaging body tissues or requiring blood collection [6], [7].

Among various non-invasive methods, photoplethysmography (PPG) has emerged as a promising optical technique for glucose estimation. PPG measures blood volume changes in microvascular tissue based on light absorption characteristics and has been widely used in physiological monitoring, including heart rate, heart rate variability, oxygen saturation, and blood pressure [8]. Because PPG can capture peripheral hemodynamic dynamics that may be influenced by glucose metabolism, this technique has been increasingly explored for non-invasive glucose estimation [9], [10]. In addition, its low cost, simplicity, and compatibility with wearable devices make PPG suitable for continuous health monitoring applications [11], [12].

Previous studies indicate that PPG contains useful physiological information for estimating blood glucose levels. As the recent studies used physiological, signal-oriented, and physical parameters derived from PPG signals collected with the SFH7050 sensor by Gupta et al. [13]. Nie et al. [9] also employed imaging photoplethysmography (IPPG) with pulse wave features for glucose prediction, while Cheng et al. [14] investigated heart rate features, the Teager–Kaiser Energy Operator, and log-energy using a visible–near-infrared light source. Other studies have explored raw PPG-based modeling [15] and Mel-Frequency Cepstral Coefficients (MFCC)-based feature extraction to capture spectral information from PPG signals [16].

However, most existing approaches still rely on raw PPG signals, pulse waveforms, or feature representations from a single domain. Despite these advancements, several limitations remain. Raw PPG-based approaches still face challenges in representing complex and time-varying hemodynamic changes, particularly those associated with fluctuations in blood glucose levels. Relying solely on raw PPG may produce representations that do not fully capture the physiological mechanisms underlying glucose-related signal variations. To address these limitations, this study explores PPG-derived signals, namely the velocity photoplethysmogram (VPG) and acceleration photoplethysmogram (APG), as complementary representations. VPG and APG provide additional information on blood flow velocity, acceleration, and vascular elasticity, thereby potentially improving model sensitivity to subtle hemodynamic variations. Therefore, this study proposes a non-invasive blood glucose estimation framework using fiducial features and MFCC-based features extracted from PPG and its derived signals. The extracted features are then modeled using a Random Forest algorithm to capture the nonlinear relationship between physiological signals and blood glucose levels. The main contributions of this study are threefold: (1) the integration of PPG-derived signals, namely VPG and APG, to enrich physiological representation; (2) the combination of fiducial and MFCC features to capture both morphological and spectral characteristics; and (3) the development of a machine learning-based estimation framework with potential applicability to wearable continuous glucose monitoring systems.

II. Theory

Non-Invasive Optical Method

Non-invasive glucose measurement approaches commonly rely on optical method based on light with biological tissues. Light at specific wavelengths undergoes absorption and scattering before being detected [17], [18]. The relationship between the incident light intensity and the detected intensity follows the Beer-Lambert law as expressed in Equation (1).

$$I = I_0 e^{-\mu_t d} \tag{1}$$

Where I_0 represents the incident light intensity, I the detected light intensity, d the optical path length within the tissue, and μ_t the total attenuation coefficient. This coefficient is composed of the absorption coefficient μ_a and the scattering coefficient μ_s, as expressed in Equation (2).

$$\mu_t = \mu_a + \mu_s \tag{2}$$

In biological tissues, scattering effect are dominant therefore the Modified Beer-Lambert law is applied, as expressed in Equation (3).

$$A = \log\left(\frac{I_0}{I}\right) = \varepsilon c l + G \tag{3}$$

Where A represents the optical absorbance, ε is the molar extinction coefficient of the chromophore, c represents the concentration of absorbing substances including glucose, l is the effective optical path length, and G is a correction factor accounting for tissue scattering. Variations in glucose concentration influence the optical properties of the tissue and are reflected in the measured signal [19].

PPG and Its Derivatives

PPG is an optical technique used to measure blood volume changes. The PPG signal can be further analyzed through its derivatives to extract more detailed physiological information. The first derivative produces the VPG, as expressed in Equation (4).

$$VPG(t) = \frac{dPPG(t)}{dt} \tag{4}$$

The second derivative produces the APG, as expressed in Equation (5).

$$APG(t) = \frac{d^2PPG(t)}{dt^2} \tag{5}$$

p-ISSN: 2621-3761
e-ISSN: 2621-2889

VPG represents the rate of change in blood volume, while APG is associated with blood flow acceleration and vascular elasticity [20].

MFCCs

MFCCs are used to represent the nonlinear spectral characteristics of physiological signals such as PPG. This method effectively captures the frequency energy distribution related to hemodynamic dynamics [16]. The initial step involves windowing using a Hamming function, as expressed in Equation (6).

$$y(n) = x(n)w(n) \tag{6}$$

The frequency is then mapped to the Mel scale, as expressed in Equation (7).

$$f_{mel} = 2595 \log\left(1 + \frac{f}{700}\right) \tag{7}$$

Finally, cepstral coefficients are obtained using the Discrete Cosine Transform (DCT), as expressed in Equation (8).

$$c(n) = \sum_{m=0}^{M-1} \log(s(m)) \cos\left(\frac{\pi n(m+0.5)}{M}\right) \tag{8}$$

III. Method

This study employed an experimental-computational research design. The experimental component involved acquiring PPG signals using a non-invasive optical sensor, while the computational component included signal preprocessing, derivative generation, feature extraction, machine learning modeling, and performance evaluation for blood glucose estimation.

A non-invasive approach based on the optical MAX30102 sensor has been developed as illustrated in Figure 1. This sensor has been widely employed for finger-based PPG signal acquisition [21]. Data collection was conducted with 58 subjects, and PPG signals were recorded at 100 Hz for 100 s per subject. For clinical reference and comparison, invasive measurements were also performed using a commercial EasyTouch glucometer to obtain ground-truth blood glucose values.

Subjects were recruited using a convenience sampling approach. The reference blood glucose measurements were obtained under pre-prandial and post-prandial conditions to capture variations in glucose levels before and after food intake. During data acquisition, each subject was instructed to remain seated and keep the finger stable on the sensor to minimize motion artifacts. Subjects with incomplete measurements or severely distorted PPG recordings were excluded from further analysis. Detailed demographic characteristics, such as age, sex, and diabetes status, were not analyzed in detail in this study and are therefore acknowledged as a methodological limitation.

The PPG signals from each subject were subsequently segmented into 10-s windows to increase the sample count. Prior to derivative computation, the raw PPG signals were preprocessed using a fourth-order Chebyshev Type II bandpass filter, which has been reported to enhance PPG signal quality [22]. Filtering was implemented with a stopband attenuation of 20 dB within the frequency range of 0.5–8 Hz. From the filtered PPG signals, first- and second-order derivatives were computed.

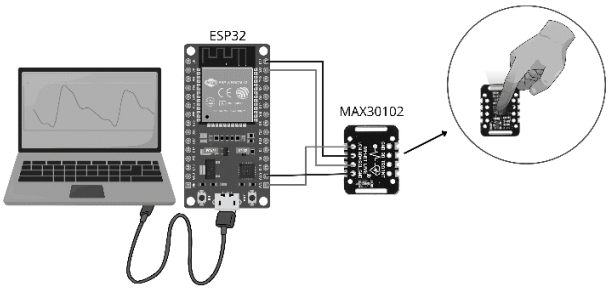

Figure 1. Data acquisition device using the MAX30102 sensor

Fiducial feature extraction was performed on the PPG, VPG, and APG signals, as illustrated in Figure 2. Two principal points (a and b) were identified in the PPG waveform, three points (a, b, and c) in the VPG waveform, and five points (a through e) in the APG waveform. All fiducial points were detected at local extrema, either peaks or troughs, corresponding to slope changes in the waveform [23].

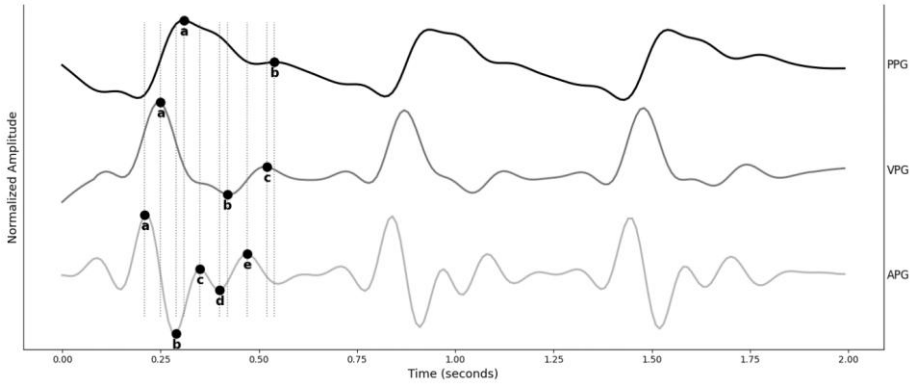

Figure 2. Fiducial points in the signals

p-ISSN: 2621-3761
e-ISSN: 2621-2889

In addition to fiducial features, spectral features were extracted using MFCCs. This process involves segmenting the signal into frames of 128 samples with a hop length of 32 samples. Each frame is then multiplied by a Hamming window to reduce spectral discontinuities. The spectral energy is subsequently projected onto the Mel scale using triangular filter banks, followed by logarithmic compression and a DCT to obtain the MFCCs coefficients.

Blood glucose estimation modeling was conducted using the Random Forest algorithm, an ensemble learning method based on decision trees that independently construct multiple trees via bootstrap sampling. For regression tasks, the final prediction is obtained by averaging the outputs of all constituent trees, thereby reducing model variance and mitigating overfitting relative to a single-tree approach. In addition, Random Forest is robust to noise and facilitates the analysis of the relative contributions of individual features to the model output [24]. The model was configured using predefined parameters, as summarized in Table 1.

Table 1. Random forest parameter

Parameter	Value
n-estimators	300
max_depth	15
min_samples_leaf	2

Model validation was performed using a hold-out validation strategy. The dataset was divided into 80% training data and 20% testing data. The training data were used to build the Random Forest model, while the testing data were used to evaluate the final prediction performance on unseen data. This validation approach was applied to assess the ability of the model to estimate blood glucose levels beyond the data used during training.

System performance was evaluated using a combination of numerical and clinical metrics, namely Mean Absolute Error (MAE), Root Mean Square Error (RMSE), Mean Absolute Relative Difference (MARD), and Clarke Error Grid Analysis (CEGA), to provide a comprehensive assessment of predictive accuracy and clinical relevance. MAE was employed to quantify the average absolute deviation between estimated and reference values, expressed in mg/dL. RMSE penalizes large errors more heavily and thus reflects overall prediction stability. MARD is expressed as a percentage and is widely used in glucose monitoring systems. CEGA was applied to assess the clinical significance of the estimation results by mapping predictions into Zones A–E, where dominance in Zones A and B indicates clinically acceptable performance.

IV. Results and Discussion

This study evaluates a non-invasive approach to estimate blood glucose from PPG signals and their derivatives, VPG and APG. After preprocessing, the signals were analyzed using two main representations: fiducial features from pulse morphology and spectral features based on MFCC. These inputs were then provided to a Random Forest model to capture peripheral hemodynamic changes linked to blood glucose fluctuations, which are nonlinear and not fully evident in the raw PPG waveform.

Differences in PPG signal characteristics before and after preprocessing are illustrated in Figure 3. The raw PPG signal showed irregular amplitude fluctuations, baseline drift, and undesirable low- and high-frequency components, which were likely caused by finger motion artifacts, sensor contact instability, and environmental noise. After applying a fourth-order Chebyshev Type II bandpass filter within the frequency range of 0.5–8 Hz, the waveform became smoother and more periodic, with clearer systolic peaks and diastolic decay phases. This improvement indicates that the filtering process successfully preserved the dominant cardiovascular components while suppressing non-physiological disturbances. A cleaner waveform is important because inaccurate peak detection may directly affect the reliability of fiducial feature extraction, especially for derivative signals such as VPG and APG, which are more sensitive to noise amplification.

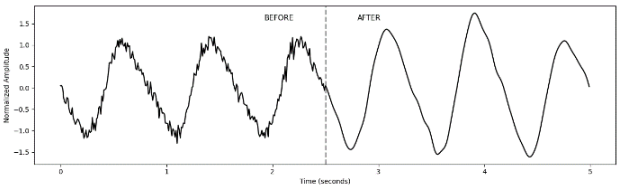

Figure 3. PPG signals before and after preprocessing

The extraction of fiducial points from PPG, VPG, and APG signals demonstrates that relevant pulse morphology information was successfully captured. In the PPG waveform, the systolic peak and diastolic peak represent blood ejection and peripheral wave reflection during early diastole. In the VPG signal, the detected characteristic points reflect changes in the slope of the PPG waveform, which are related to blood flow velocity within one cardiac cycle. Meanwhile, the APG signal provides second-order information associated with acceleration and deceleration of blood volume changes, which may reflect vascular elasticity, arterial stiffness, and peripheral resistance. Therefore, the use of derivative signals is physiologically meaningful because glucose-related changes may not only affect the amplitude of the PPG waveform but may also influence vascular tone, microcirculatory dynamics, and pulse wave propagation. Collectively, the fiducial points extracted from PPG, VPG, and APG produced 20 amplitude- and temporal-based features.

p-ISSN: 2621-3761
e-ISSN: 2621-2889

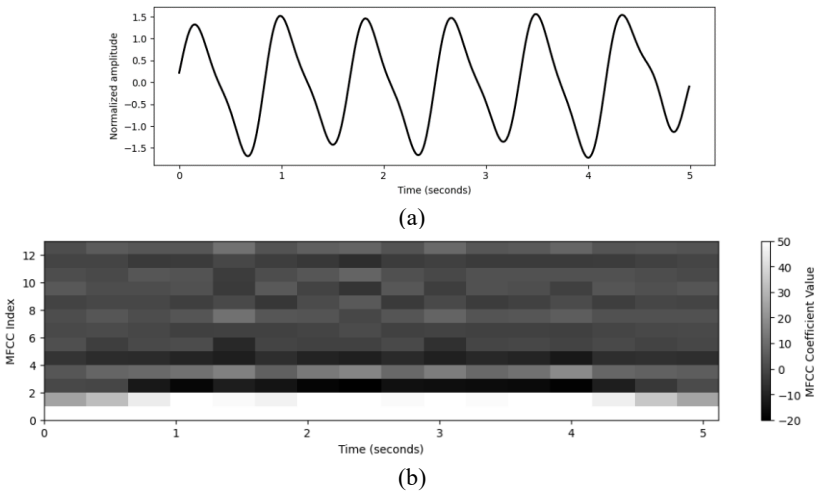

Figure 4. (a) Preprocessed PPG signal and (b) MFCCs coefficients map in the time-frequency domain

Table 2. Blood glucose estimation performance for different signal combinations

Feature	MAE (mg/dL)	RMSE (mg/dL)	MARD (%)
PPG	6.39	9.96	6.08
VPG	6.47	9.82	6.17
APG	6.75	9.87	6.49
PPG+VPG	6.42	9.87	6.12
PPG+APG	6.51	9.85	6.16
VPG+APG	6.49	9.79	6.21
PPG+VPG+APG	6.35	9.74	6.07

The performance of the Random Forest model under different signal combinations is reported in Table 2. The combination of PPG, VPG, and APG achieved the best performance, with an MAE of 6.35 mg/dL, RMSE of 9.74 mg/dL, and MARD of 6.07%. This result suggests that the original PPG signal alone may not contain sufficient information to fully represent blood glucose-related physiological changes. The addition of VPG and APG improved the model performance because these derivative signals provide complementary information regarding blood flow velocity and acceleration patterns. The improved accuracy may be due to a richer representation of peripheral hemodynamic responses when morphological, velocity-related, and acceleration-related features are combined. This finding supports the assumption that blood glucose variation may influence peripheral circulation through complex and nonlinear mechanisms, which are better captured using multiple signal representations rather than a single waveform [25].

The MFCC features also contributed to the approach's performance by capturing the spectral characteristics of the PPG-derived signals. While fiducial features describe specific time-domain pulse morphology, MFCCs summarize frequency-domain patterns that may not be directly observable from peak-based measurements. The combination of fiducial and MFCC features therefore enables the model to learn both local morphological changes and broader spectral patterns.

The clinical relevance of the estimation results was further examined using CEGA, as shown in Figure 5. The distribution of predictions indicates that 97.44% of the points fell within Zone A and 2.56% within Zone B, with all predictions residing in clinically acceptable regions. The predominance of Zone A indicates that most estimates were very close to reference values, whereas the small proportion in Zone B represents minor deviations unlikely to influence clinical decision-making. These findings confirm that the approach is not only statistically robust but also demonstrates practical potential for non-invasive blood glucose monitoring.

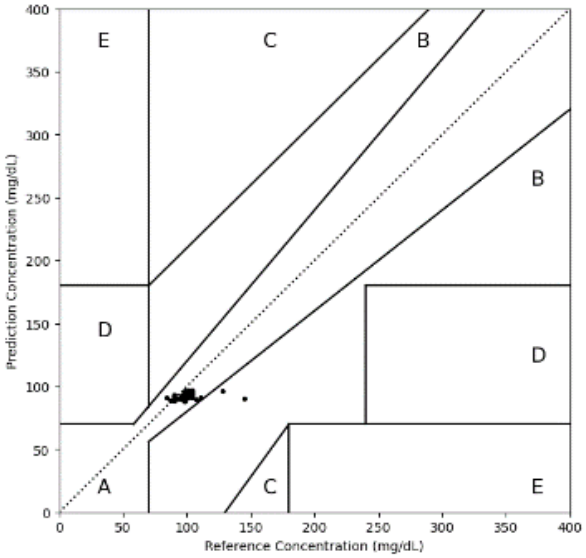

Figure 5. Distribution of glucose predictions on the CEGA

p-ISSN: 2621-3761
e-ISSN: 2621-2889

A summary of the comparison with previous studies is presented in Table 3. Compared with Study [9], which reported an MAE of 30.96 mg/dL, an RMSE of 8.90 mg/dL, and an MARD of 22.25% using IPPG pulse waveform data, the method achieved substantially lower MAE and MARD. This difference may be related to the use of derivative signals and combined fiducial-MFCC features, which provide a more complete representation of pulse dynamics. Compared with Study [16], which used two MFCC variants and achieved MAE and RMSE of 9.85 mg/dL and 16.66 mg/dL, respectively, the method also showed lower estimation errors. This suggests that MFCC features may be more effective when combined with physiologically interpretable fiducial features rather than used alone. Compared with Study [14], which used HR, TKEO, and log-energy features and reported an MAE of 11.16 mg/dL and an RMSE of 14.60 mg/dL, the approach also demonstrated better

The results indicate that combining PPG, VPG, and APG signals with fiducial and MFCC features is a promising approach for non-invasive blood glucose estimation. The method achieved competitive performance compared with previous PPG-based studies and demonstrated clinically acceptable predictions based on CEGA analysis. However, further investigation with larger datasets, broader glucose ranges, more subjects, and stronger statistical validation is required before the method can be considered reliable for practical wearable-based glucose-monitoring applications.

Table 3. Comparison of the approach with previous studies

Reference	Dataset	Range Glucose (mg/dL)	Features	Result			
				MAE (mg/dL)	RMSE (mg/dL)	MARD (mg/dL)	CEGA (%)
[13]	Self-collected using SFH7050 sensor	84-199	Physiological, signal oriented characteristic, and physical parameter	8.31	-	-	A = 96.15 B = 2.85
[9]	Self-collected IPPG using NIR camera	70-150	Pulse waveform	30.96	8.90	22.25	A = 89.60 B = 10.40
[16]	Self-collected dataset	50-400	Two MFCCs variants	9.85	16.66	-	A = 92.10 B = 5.82
[15]	VitalDB and MUST datasets	0-400	Raw PPG	14.80	19.70	-	A = 76.60 B = 32.40
[14]	Self-collected using photodiode with Vis-NIR light source	70-167	HR, TKEO & Log-energy	11.16	14.60	-	A = 95.09 B = 4.91
Our Study	Self-collected using MAX30102	70-150	PPG, VPG, and APG fiducial with MFCCs	6.35	9.74	6.07	A = 97.44 B = 2.56

V. Conclusion

This study demonstrates that integrating fiducial morphology features and MFCC-based spectral representations from PPG and its derivatives provides a promising framework for non-invasive blood glucose estimation. The main scientific contribution of this work lies in the systematic use of PPG, VPG, and APG signals within a unified feature-extraction and machine-learning framework, enabling the comprehensive representation of both morphological and spectral characteristics of peripheral hemodynamics. The best performance was achieved with the combined PPG, VPG, and APG signals and the Random Forest model, yielding MAE, RMSE, and MARD values of 6.35 mg/dL, 9.74 mg/dL, and 6.07%, respectively. In addition, CEGA showed that all predicted values were located in clinically acceptable regions, with 97.44% in Zone A and 2.56% in Zone B. These findings indicate that derivative-based PPG representations can provide complementary physiological information on blood flow velocity, acceleration, and vascular responses, thereby improving glucose estimation compared with PPG alone. Despite these promising results, this study has several limitations, including the use of a self-collected dataset with a relatively small number of subjects and a narrow glucose range. Therefore, future research should involve larger, more diverse datasets and a wider range of glucose concentrations. Further studies may also explore deep learning approaches and the development of real-time wearable systems for continuous non-invasive blood glucose monitoring.

p-ISSN: 2621-3761
e-ISSN: 2621-2889

References

[1] M. J. Hossain, M. Al-Mamun, and M. R. Islam, "Diabetes mellitus, the fastest growing global public health concern: Early detection should be focused," *Heal. Sci. Reports*, vol. 7, no. 3, Mar. 2024, doi: 10.1002/hsr2.2004.

[2] International Diabetes Federation, *Atlas Diabetes 2025*, 11th ed. 2025. [Online]. Available: https://diabetesatlas.org/resources/idf-diabetes-atlas-2025/

[3] International Diabetes Federation, "IDF global clinical practice recommendations for managing type 2 diabetes – 2025," 2025. doi: 10.1016/j.diabres.2025.112152.

[4] M. Farouk, A. S. A. El-Hameed, A. R. Eldamak, and D. N. Elsheakh, "Noninvasive blood glucose monitoring using a dual band microwave sensor with machine learning," *Sci. Rep.*, vol. 15, no. 1, p. 16271, May 2025, doi: 10.1038/s41598-025-94367-6.

[5] N. Uluç *et al.*, "Non-invasive measurements of blood glucose levels by time-gating mid-infrared optoacoustic signals," *Nat. Metab.*, vol. 6, no. 4, pp. 678–686, Mar. 2024, doi: 10.1038/s42255-024-01016-9.

[6] Q. Gong *et al.*, "Non-Invasive and Accurate Blood Glucose Detection Based on an Equivalent Bioimpedance Spectrum," *Appl. Sci.*, vol. 15, no. 3, p. 1266, Jan. 2025, doi: 10.3390/app15031266.

[7] S.-E. Jian, Y.-L. Lo, Y.-T. Chuang, and S.-H. Kuo, "Using Machine learning to predict blood glucose level based on Photoplethysmography," *Measurement*, vol. 253, p. 117421, Sep. 2025, doi: 10.1016/j.measurement.2025.117421.

[8] E. Mejía-Mejía, J. Allen, K. Budidha, C. El-Hajj, P. A. Kyriacou, and P. H. Charlton, *Photoplethysmography signal processing and synthesis*. 2021. doi: 10.1016/B978-0-12-823374-0.00015-3.

[9] Z. Nie, M. Rong, and K. Li, "Blood glucose prediction based on imagingphotoplethysmography in combination with Machine learning," *Biomed. Signal Process. Control*, vol. 79, p. 104179, Jan. 2023, doi: 10.1016/j.bspc.2022.104179.

[10] J. Chu, W.-T. Yang, W.-R. Lu, Y.-T. Chang, T.-H. Hsieh, and F.-L. Yang, "90% Accuracy for Photoplethysmography-Based Non-Invasive Blood Glucose Prediction by Deep Learning with Cohort Arrangement and Quarterly Measured HbA1c," *Sensors*, vol. 21, no. 23, p. 7815, Nov. 2021, doi: 10.3390/s21237815.

[11] G. Hammour and D. P. Mandic, "An In-Ear PPG-Based Blood Glucose Monitor: A Proof-of-Concept Study," *Sensors*, vol. 23, no. 6, p. 3319, Mar. 2023, doi: 10.3390/s23063319.

[12] S. Alghlayini, M. A. Al-Betar, and M. Atef, "Enhancing Non-Invasive Blood Glucose Prediction from Photoplethysmography Signals via Heart Rate Variability-Based Features Selection Using Metaheuristic Algorithms," *Algorithms*, vol. 18, no. 2, p. 95, Feb. 2025, doi: 10.3390/a18020095.

[13] S. Sen Gupta, T.-H. Kwon, S. Hossain, and K.-D. Kim, "Towards non-invasive blood glucose measurement using machine learning: An all-purpose PPG system design," *Biomed. Signal Process. Control*, vol. 68, p. 102706, Jul. 2021, doi: 10.1016/j.bspc.2021.102706.

[14] J. Cheng, P. Xie, H. Zhao, and Z. Ji, "Differential Absorbance and PPG-Based Non-Invasive Blood Glucose Measurement Using Spatiotemporal Multimodal Fused LSTM Model," *Sensors*, vol. 25, no. 17, p. 5260, Aug. 2025, doi: 10.3390/s25175260.

[15] M. Zeynali, K. Alipour, B. Tarvirdizadeh, and M. Ghamari, "Non-invasive blood glucose monitoring using PPG signals with various deep learning models and implementation using TinyML," *Sci. Rep.*, vol. 15, no. 1, p. 581, Jan. 2025, doi: 10.1038/s41598-024-84265-8.

[16] C. Salamea-Palacios, M. Montalvo-López, R. Orellana-Peralta, and J. Viñanzaca-Figueroa, "Photoplethysmography Feature Extraction for Non-Invasive Glucose Estimation by Means of MFCC and Machine Learning Techniques," *Biosensors*, vol. 15, no. 7, p. 408, Jun. 2025, doi: 10.3390/bios15070408.

[17] A. Zilgarayeva *et al.*, "Optical sensor to improve the accuracy of non-invasive blood sugar monitoring," *Indones. J. Electr. Eng. Comput. Sci.*, vol. 34, no. 3, p. 1489, Jun. 2024, doi: 10.11591/ijeecs.v34.i3.pp1489-1498.

[18] D. Di Filippo, F. Sunstrum, J. Khan, and A. Welsh, "Non-Invasive Glucose Sensing Technologies and Products: A Comprehensive Review for Researchers and Clinicians," *Sensors*, vol. 23, no. 22, p. 9130, Nov. 2023, doi: 10.3390/s23229130.

[19] I. Oshina and J. Spigulis, "Beer–Lambert law for optical tissue diagnostics: current state of the art and the main limitations," *J. Biomed. Opt.*, vol. 26, no. 10, Oct. 2021, doi: 10.1117/1.JBO.26.10.100901.

[20] M. Elgendi, Y. Liang, and R. Ward, "Toward Generating More Diagnostic Features from Photoplethysmogram Waveforms," *Diseases*, vol. 6, no. 1, p. 20, Mar. 2018, doi: 10.3390/diseases6010020.

[21] S. Ali *et al.*, "Development and Evaluation of a Sensor-Based Non-Invasive Blood Glucose Monitoring System Using Near-Infrared Spectroscopy," in *ICSEE 2024*, Basel Switzerland: MDPI, Nov. 2024, p. 19. doi: 10.3390/ecsa-11-20395.

[22] Y. Liang, M. Elgendi, Z. Chen, and R. Ward, "An optimal filter for short photoplethysmogram signals," *Sci. Data*, vol. 5, no. 1, p. 180076, May 2018, doi: 10.1038/sdata.2018.76.

[23] M.-S. Song and S.-B. Lee, "Interpretable machine learning for hypertension detection using photoplethysmography (PPG) signals and their derivatives," *Biomed. Signal Process. Control*, vol. 113, p. 109194, Mar. 2026, doi: 10.1016/j.bspc.2025.109194.

[24] G. A. Alonso-Silverio, V. Francisco-García, I. P. Guzmán-Guzmán, E. Ventura-Molina, and A. Alarcón-Paredes, "Toward Non-Invasive Estimation of Blood Glucose Concentration: A Comparative Performance," *Mathematics*, vol. 9, no. 20, p. 2529, Oct. 2021, doi: 10.3390/math9202529.

[25] X. Hu *et al.*, "Blood pressure stratification using photoplethysmography and light gradient boosting machine," *Front. Physiol.*, vol. 14, Feb. 2023, doi: 10.3389/fphys.2023.1072273.

p-ISSN: 2621-3761
e-ISSN: 2621-2889

Declarations

Author contribution : Ferdyan Rahmadani Adhi Pramudya contributed to conceptualization, methodology, and writing the original draft. Muhammad Bagoes Anargiansyah was responsible for software development and data curation. Bilqis Regita Pratiwi Fayensi handled project administration. Moh Khikam Amrullah provided resources. Nisa'ul Fadhilah conducted formal analysis. Nainunis Mutawakkillah carried out the investigation. Muhimmatul Khoiro contributed to writing—review and editing, as well as validation and supervision.

Funding statement : This research did not receive any funding.

Conflict of interest : All authors declare that they have no competing interests.

Additional information : No additional information is available for this paper.

p-ISSN: 2621-3761
e-ISSN: 2621-2889